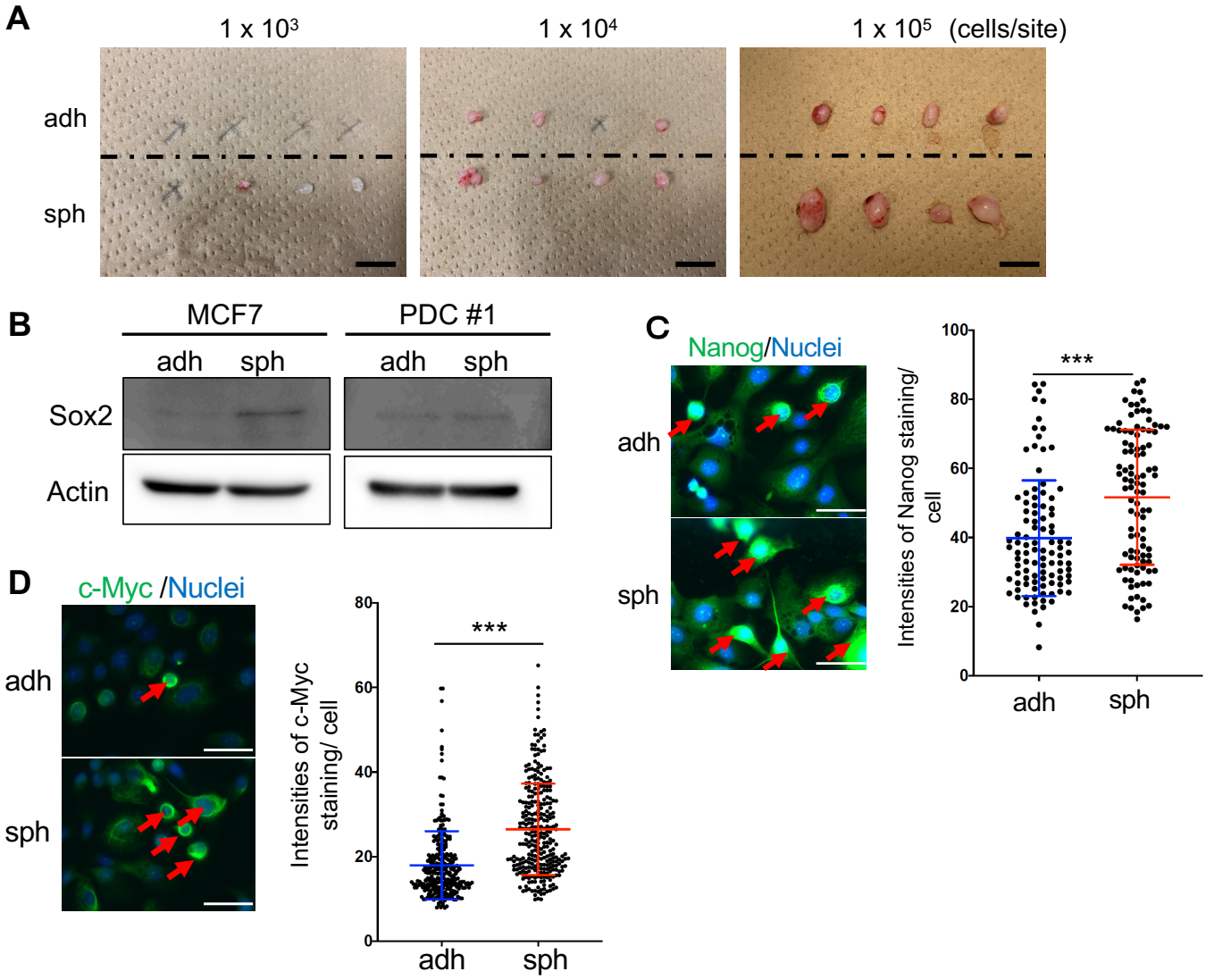

Figure S1. CSCs are enriched in sphere culture population. A, Representative images of tumors formed in the *in vivo* limiting dilution assay (1 × 10^3, 10^4 and 10^5 cells/site). Scale bar = 10 mm. **B**, Expression levels of Sox2 in MCF7 and PDC #1 cells were compared between cells cultured under adherent and sphere conditions. Actin was used for loading control. **C**, (Left) Immunofluorescence images of Nanog staining in PDC #1 cells cultured under adherent and sphere conditions are shown. Nuclei were counterstained with DAPI. Arrows indicate cells with strong Nanog staining. Scale bar = 50 μm. (Right) The intensities of Nanog staining were quantified by using ImageJ software. One hundred cells in each slide were counted (mean ±SD, n = 3; ***$p < 0.001$). **D**, (Left) Immunofluorescence images of Myc staining in PDC #1 cells cultured under adherent and sphere conditions are shown. Nuclei were counterstained with DAPI. Arrows indicate cells with strong Myc staining. Scale bar = 50 μm. (Right) The intensities of Myc staining were quantified by using ImageJ software. One hundred cells in each slide were counted (mean ±SD, n = 3; ***$p < 0.001$).

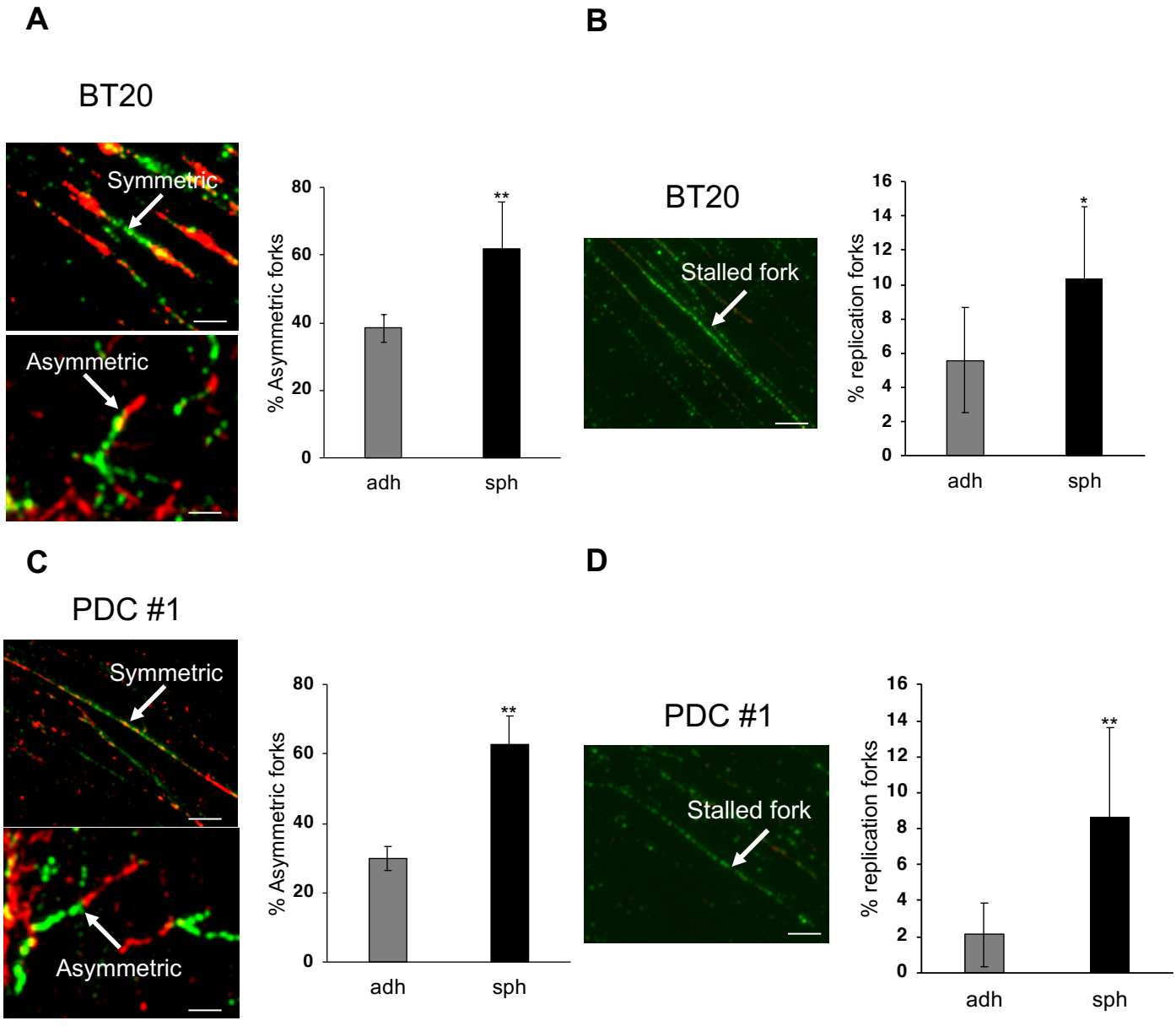

Figure S2. DNA replication stress is upregulated in CSC-enriched spheroid cells. A,C, Proportion of asymmetric forks, representative of replication stress. Thirty bidirectional forks in each slide were counted. Three slides for each population were prepared (mean ± SEM, n = 3; **p < 0.01). Scale bar = 10 μm. **B, D**, Proportion of stalled forks, labeled only with green was calculated. Two hundred labeled forks in each slide were counted. Three slides for each population were prepared (mean ± SEM, n = 3; **p < 0.01). Scale bar = 5 μm.

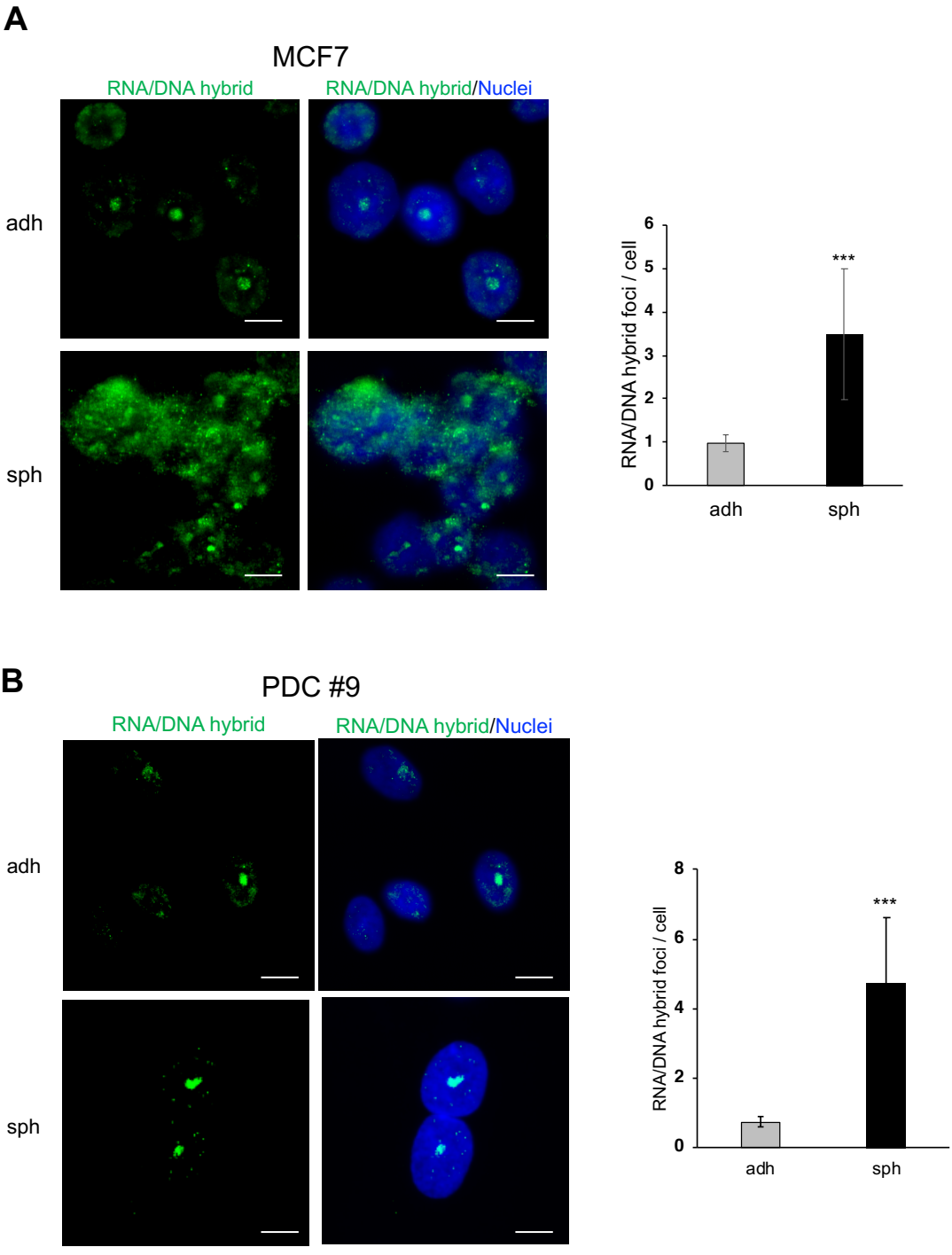

Figure S3. RNA/DNA hybrid foci are increased in spheroid cells. A, B, (Left) Immunofluorescence images of RNA/DNA hybrid staining in cells cultured in the adherent and sphere conditions are shown. (Right) Number of RNA/DNA hybrid foci in each cell was counted and compared between the two conditions. Hundred cells in each slide were counted. Three slides for each population were prepared (mean ± SEM, n = 3; ***$p < 0.001$). Scale bar = 10 μm.

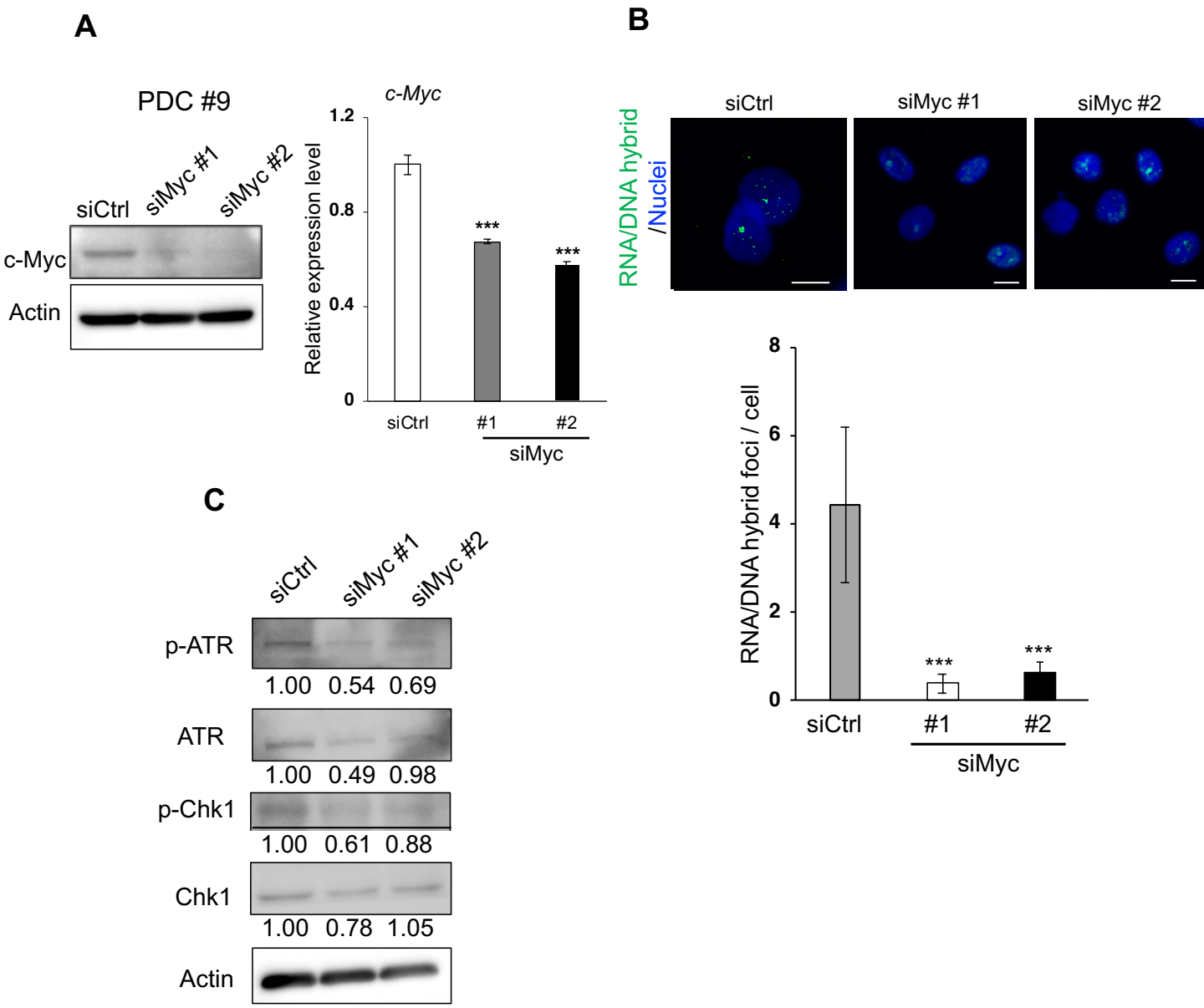

Figure S4. c-Myc expression contributes to replication stress. A, Knockdown efficiencies of siRNAs targeting *c-Myc* (siMyc #1 and #2) or control siRNA (siCtrl) in PDC#9 was compared by immunoblotting (left) and qPCR (right) (mean ± SEM, n = 3; ***p < 0.001). **B**, Number of RNA/DNA hybrid foci in each cell was counted and compared among spheroid cells treated with siCtrl, *siMyc* #1, and *siMyc* #2. Scale bar = 10 μm. Hundred cells in each slide were counted. Three slides for each population were prepared (mean ± SEM, n = 3; ***p < 0.001). **C**, Expression levels of ATR, p-ATR, Chk1 and p-Chk1 as determined by immunoblotting, were compared among cells treated with siCtrl, *siMyc* #1, and *siMyc* #2. Expression was quantified by ImageJ and normalized to Actin.

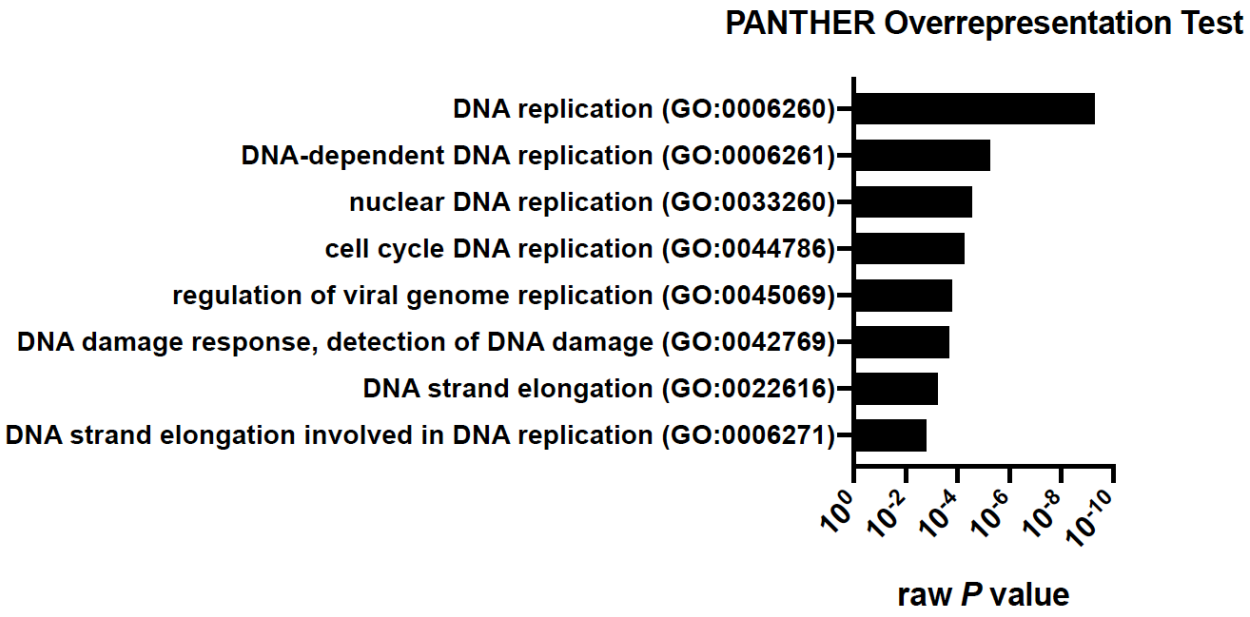

Figure S5. Gene Ontology (GO) enrichment analysis (http://pantherdb.org/about.jsp). Genes of which expression levels are >1.5 fold in spheroid cells than in adherent cells were analyzed.

.

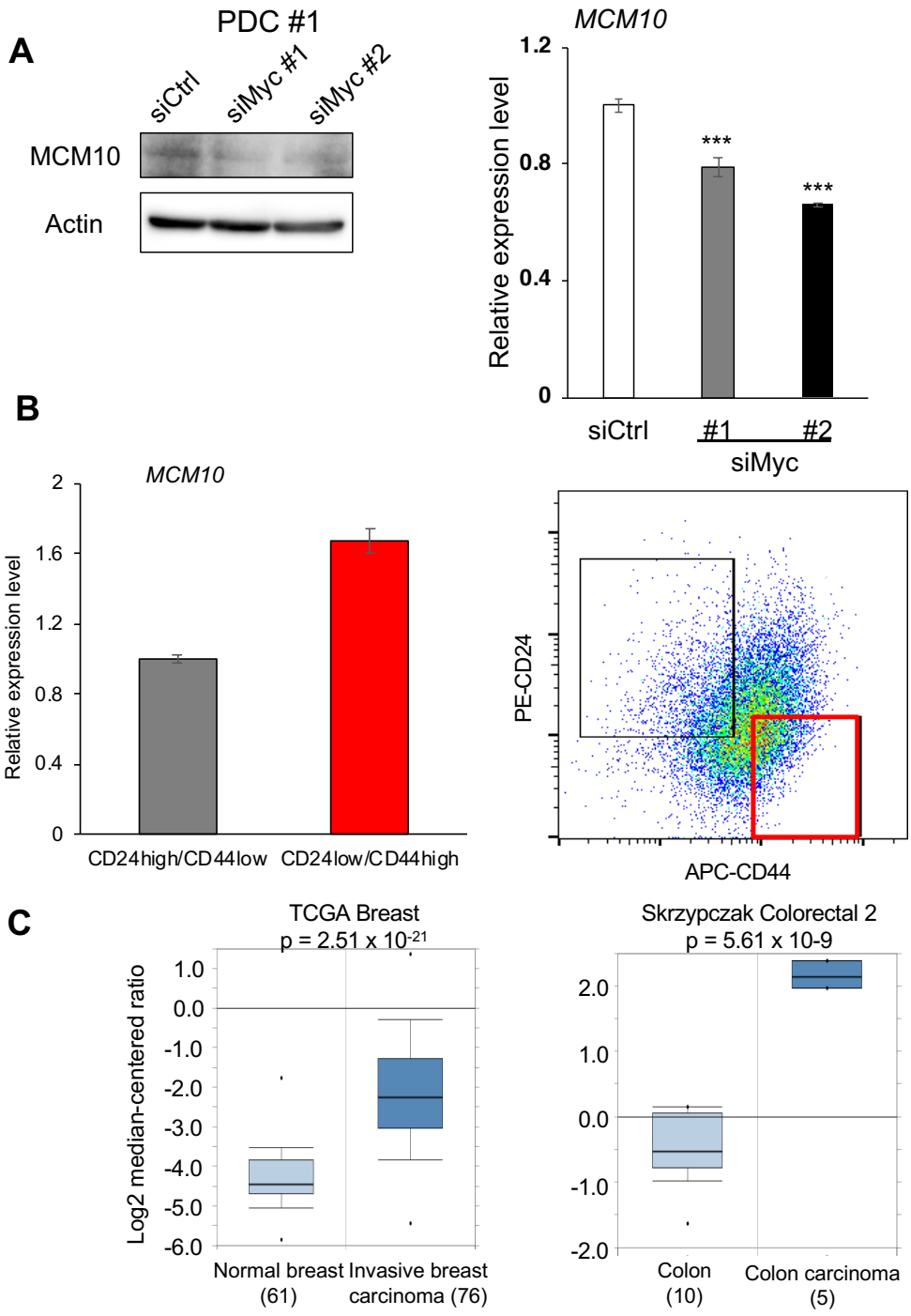

Figure S6. MCM10 expression is associated with c-Myc expression and upregulated in cancer stem-like cells and in cancer tissues. A, Expression level of MCM10 in PDC#1 in sphere conditions treated with siCtrl, *siMyc* #1 and *siMyc* #2 was compared by immunoblotting (left) and qPCR (right) (mean ± SEM, n = 3; ***p < 0.001). Actin was used for loading control. **B,** Expression level of *MCM10* was compared by qPCR between the $CD24^{-/low}/CD44^{high}$ CSC-enriched population and the $CD24^{high}/CD44^{low}$ control population. The PDC #6 cells were analyzed. (mean ± SEM, n = 3; *p < 0.05). **C**, *MCM10* expression was compared between non-malignant cells and cancer cells in breast and colon using the Oncomine cancer gene expression database (Left; TCGA Breast, Right; Skrzypczak Colorectal 2). P-values were calculated by Student's t-test.

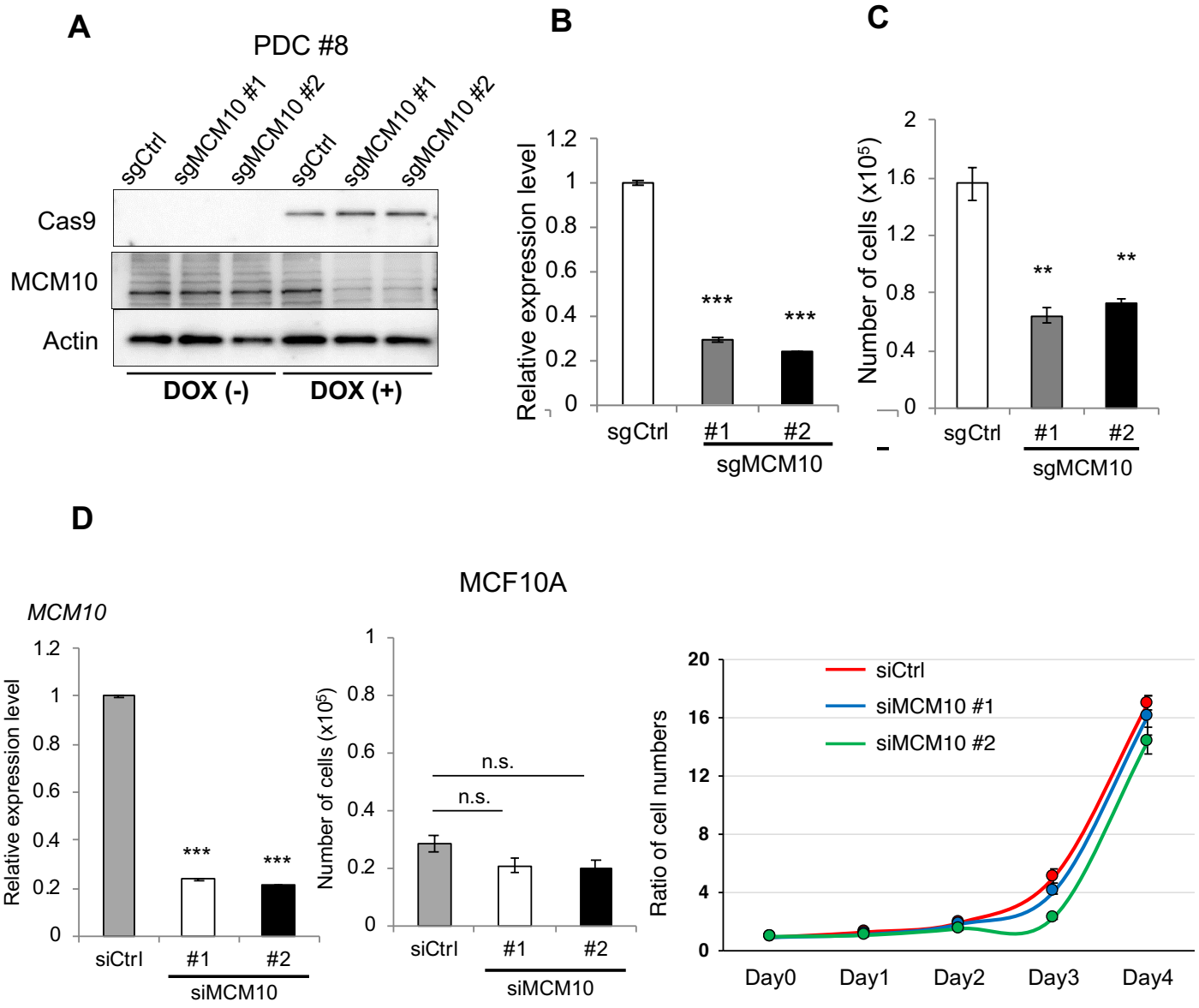

Figure S7. MCM10 plays important roles for proliferation of cancer cells. A, B, DOX-inducible knockout in PDC #8 (sgMCM10) and control cells (shCtrl) were compared by immunoblotting (**A**) and qPCR (**B**) (mean ± SEM, n = 3; ***p < 0.001). **C**, Cells were seeded in 12-well plates (10,000 cells/well) and cultured. Then they were harvested and counted after 4 days (mean ± SEM, n = 3; **p < 0.01). **D,** MCF10A treated with siCtrl or *siMCM10*. Knockdown efficiencies of siRNAs (left) and cell proliferation (middle and right) were compared.

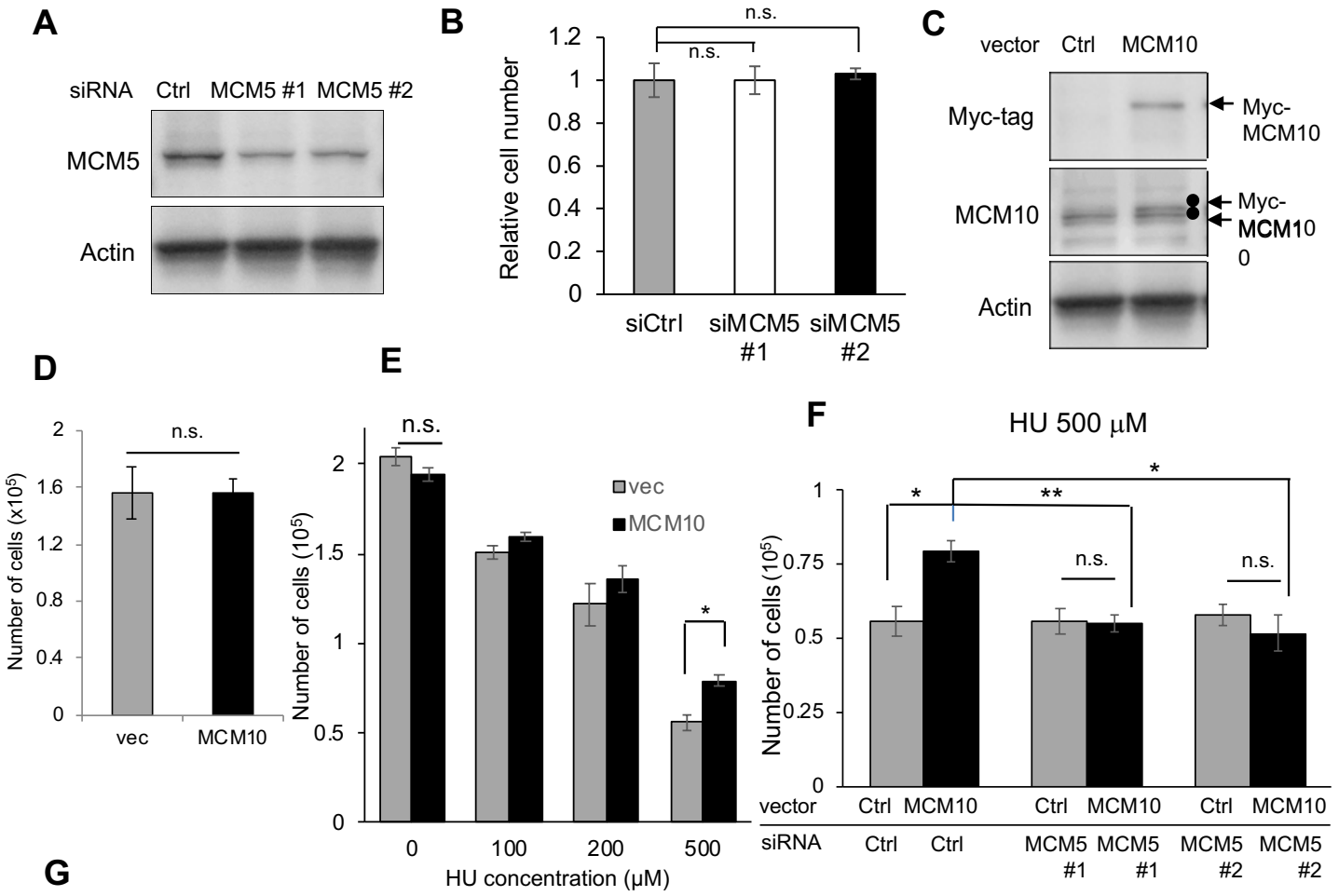

G

In vitro limiting dilution assay

	Cells (per site)						CSC frequency	Probability (vs shCtrl)
	63	125	250	500	1000	2000		
shCtrl	0/8	1/8	5/8	7/8	8/8	8/8	1/319	-
shMCM10 #1	0/8	0/8	1/8	4/8	8/8	8/8	1/652	0.0456
shMCM10 #2	0/8	0/8	1/8	3/8	8/8	8/8	1/716	0.0241

Figure S8. MCM5 is involved in the functions of MCM10 and MCM10 plays important roles for sphere formation in vitro. A, B, Expression levels of MCM5 were compared in MCF7 cells treated with siCtrl or *siMCM5* (**A**). Number of cells were counted after 4 days (mean ± SEM, n = 3) (**B**). **C,D**, Expression levels of endogenous MCM10 and Myc-tagged MCM10, as determined by immunoblotting, were compared among cells transfected with the indicated expression vectors (**C**). Number of cells were counted after 4 days (mean ± SEM, n = 3)(**D**). **E,F,** MCF7 cells were transfected with the Myc-tagged MCM10 or empty vector (**E**). MCF7 cells were transfected with the Myc-tagged MCM10 or empty vector with indicated siRNAs (**F**). Cells were seeded in a 12-well plate (10,000 cells/well). Forty-eight hours later, they were treated with indicated concentrations of HU for an additional 48 h. Cells were harvested and counted (mean ± SEM, n = 3; $^{**}p < 0.01$, $^{*}p < 0.05$). **G**, In vitro limiting dilution assay for MCM10-depleted cells in patient-derived breast cancer cells: 2,000, 1,000, 500, 250, 125, or 63 cells were seeded in each well of a 96-well ultra–low-attachment plates. Results were obtained 7 days after seeding. CSC frequency and p-values were determined using the ELDA software.

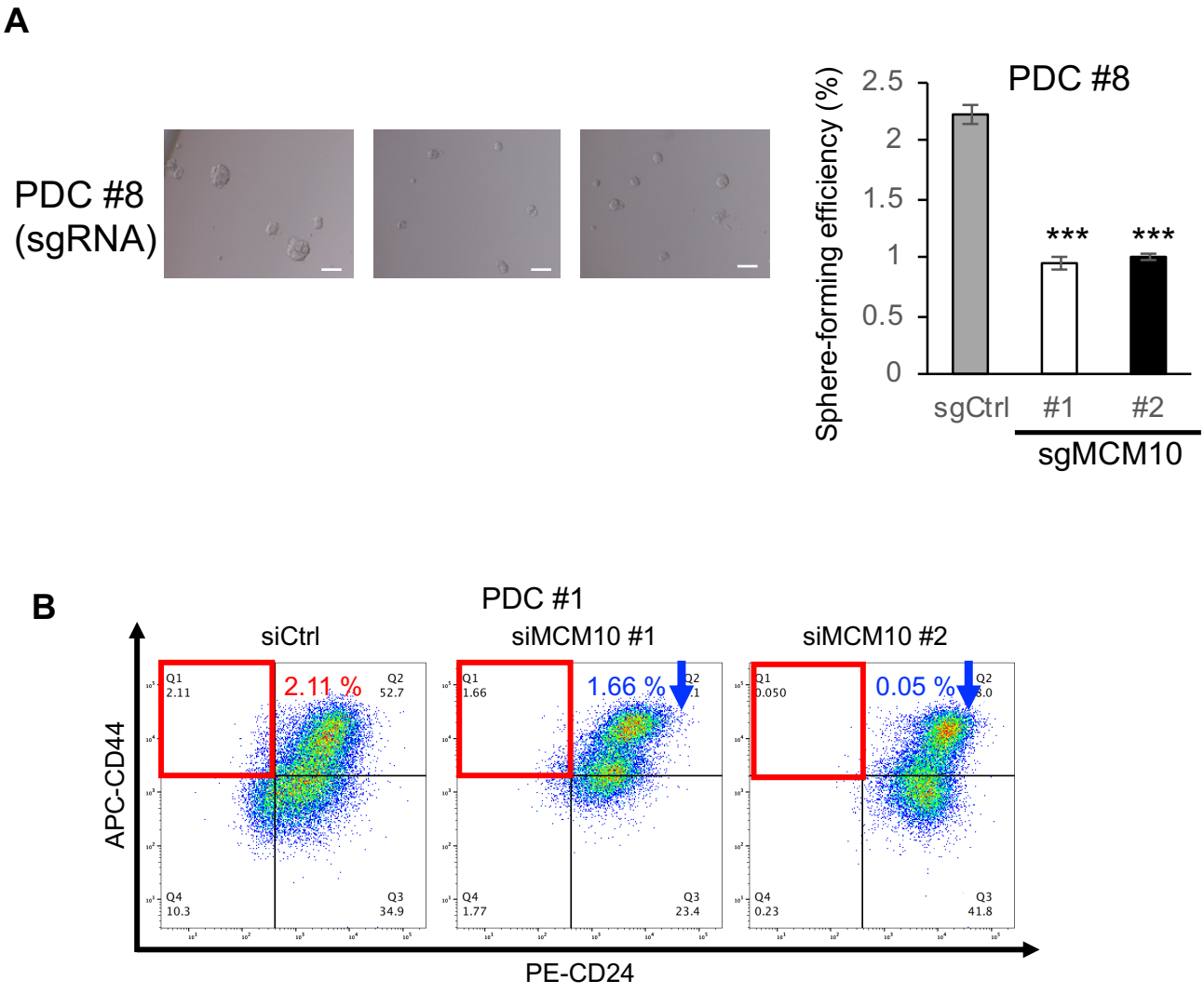

Figure S9. MCM10 plays important roles for CSC properties. A (Left) Representative images of tumor spheres. DOX-inducible *MCM10* knockout PDC #8 cells were cultured under sphere conditions. Scale bar = 100 μm. (Right) Quantification of tumor sphere formation efficiency. Spheres were formed for 6 days (mean ± SEM, n = 4; ***p < 0.001). **B**, PDC#1 treated with siCtrl, *siMCM10* #1 or *siMCM10* #2 were stained with CD44 and CD24 antibodies, and then subjected to flow cytometry analysis.

Table S1. Characteristics of clinical breast tumors used in this study

PDC (#)	ER	PgR	HER2	Molecular subtypes
1	-	-	0	Triple negative
2	3+	3+	2+ (FISH+)	Luminal HER2
3	3+	-	3+	Luminal HER2
4	-	-	2+ (FISH+)	HER2
5	-	-	2+ (FISH-)	Luminal like
6	+	+	2+ (FISH-)	Luminal like
7	-	+	-	Luminal like
8	-	-	-	Ovarian cancer
9	+	+	-	Luminal like

Table S2. Genes included in Reactome_DNA_Replication gene set and the ratios of expression levels of each gene, sphere cells (SPH) / adherent cells (ADH)

Rank	Gene symbol	SPH/ADH
1	GMNN	37.044
2	SPC25	28.289
3	RPS27A	27.516
4	PSME1	21.896
5	MCM10	15.916
6	CDT1	15.123
7	PSMC2	13.974
8	CENPI	13.831
9	AURKB	12.728
10	CDC6	12.029
11	BIRC5	9.943
12	GINS2	9.823
13	SKA1	9.493
14	NDC80	9.282
15	CENPM	8.938
16	ERCC6L	8.639
17	PSMD9	8.307
18	NUF2	7.717
19	CDC45	7.440
20	KIF2C	7.041
21	NUDC	7.037
22	PRIM1	6.714
23	ZWINT	6.504
24	CDCA8	6.473
25	CENPK	6.246
26	MLF1IP	5.954
27	ZWILCH	5.924
28	KIF18A	5.346
29	GINS1	5.281
30	FEN1	5.251
31	E2F1	4.845
32	GORASP1	4.819
33	CENPA	4.714
34	PLK1	4.472
35	SGOL2	4.429
36	BUB1	4.375
37	E2F2	4.169
38	ITGB3BP	4.135
39	TAOK1	3.893
40	PCNA	3.872
41	ORC6	3.823
42	SMC3	3.778
43	MCM5	3.717
44	CENPQ	3.709
45	SGOL1	3.628
46	RFC3	3.606
47	CDC7	3.542
48	KIF23	3.485
49	APITD1	3.353
50	BUB1B	3.351
51	CENPL	3.325
52	ORC1	3.265
53	RFC2	3.244
54	PPP2R5B	3.204
55	CDC20	3.180
56	MCM4	3.153
57	RANBP2	3.138
58	MCM6	3.083
59	CENPN	3.048
60	PPP2R5A	2.991
61	INCENP	2.967
62	MCM7	2.926
63	POLD3	2.837
64	CASC5	2.796
65	PSMA1	2.785
66	KIF20A	2.776
67	RAD21	2.735
68	DNA2	2.724
69	LIG1	2.710
70	CENPP	2.706
71	SKA2	2.696
72	SPC24	2.657
73	PPP2CB	2.635
74	MAD2L1	2.634
75	FBXO5	2.612
76	CDKN1A	2.611
77	RPA3	2.554
78	CCNA1	2.552
79	CENPO	2.513
80	DSN1	2.460
81	MCM3	2.456
82	NUP85	2.418
83	PSMF1	2.379
84	DBF4	2.332
85	MCM8	2.249
86	POLE	2.223
87	PSMC4	2.145
88	SEC13	2.123
89	MCM2	2.109
90	STAG1	1.914
91	PSMA8	1.895
92	PPP2R1A	1.836
93	NUP133	1.833
94	SMC1A	1.804
95	PSMC5	1.799
96	PPP2R5E	1.790
97	ORC2	1.776
98	PSMD10	1.773
99	NUP37	1.771
100	BUB3	1.767
101	NSL1	1.746
102	PSMC3	1.743
103	PSMA3	1.739
104	PMF1	1.733
105	RPA2	1.720
106	PSMA5	1.707
107	PSMD11	1.700
108	RPA1	1.698
109	CENPT	1.646
110	PSMB7	1.645
111	PSMD12	1.644
112	PSMD1	1.634
113	PSMA2	1.616
114	PAFAH1B1	1.608
115	PSMD6	1.595
116	POLD2	1.564
117	PSMA7	1.533
118	RFC4	1.528
119	POLA2	1.519
120	CLIP1	1.509
121	PSME2	1.509
122	POLE2	1.489
123	PSMB1	1.467
124	UBA52	1.466
125	CCNA2	1.461
126	PSMB5	1.451
127	ORC4	1.405
128	PSMD14	1.402
129	PSMD8	1.377
130	ORC3	1.366
131	PSMB8	1.352
132	PSMD13	1.344
133	PSMD2	1.336
134	MIS12	1.320
135	XPO1	1.316
136	PSMD4	1.282
137	GINS4	1.275
138	NUP107	1.271
139	CENPH	1.269
140	PSMA6	1.253
141	ORC5	1.211
142	ZW10	1.187
143	PRIM2	1.182
144	PSMB9	1.167
145	PSMB6	1.157
146	NUP43	1.156
147	POLA1	1.147
148	PSMD7	1.138
149	RB1	1.131
150	AHCTF1	1.129
151	PSMA4	1.128
152	PSMB3	1.114
153	CDKN1B	1.108
154	PPP2R5C	1.108
155	PPP2CA	1.105
156	PPP2R1B	1.103
157	CDK2	1.094
158	PPP1CC	1.020
159	MAD1L1	0.989
160	PPP2R5D	0.896
161	PSMD3	0.885
162	PSMB4	0.880
163	MAPRE1	0.868
164	PSMB10	0.844
165	KIF2A	0.822
166	KNTC1	0.814
167	E2F3	0.773
168	PSMD5	0.768
169	STAG2	0.766
170	POLD4	0.695
171	SEH1L	0.626
172	PSMB2	0.624
173	PSMC6	0.610
174	RFC5	0.548
175	PSME4	0.533
176	RCC2	0.502
177	CKAP5	0.496
178	NDEL1	0.472
179	CLASP1	0.438
180	RANGAP1	0.436
181	CENPC1	0.417
182	B9D2	0.320
183	PSMC1	0.121
184	RPS27	0.020